

# Optical Engineering

OpticalEngineering.SPIEDigitalLibrary.org

## Study on verifying the angle measurement performance of the rotary-laser system

Jin Zhao  
Yongjie Ren  
Jiarui Lin  
Shibin Yin  
Jigui Zhu

Jin Zhao, Yongjie Ren, Jiarui Lin, Shibin Yin, Jigui Zhu, "Study on verifying the angle measurement performance of the rotary-laser system," *Opt. Eng.* **57**(4), 044106 (2018), doi: 10.1117/1.OE.57.4.044106.

**SPIE.**

# Study on verifying the angle measurement performance of the rotary-laser system

Jin Zhao, Yongjie Ren,\* Jiarui Lin, Shibin Yin, and Jigui Zhu

Tianjin University, State Key Laboratory of Precision Measuring Technology and Instruments, Tianjin, China

**Abstract.** An angle verification method to verify the angle measurement performance of the rotary-laser system was developed. Angle measurement performance has a great impact on measuring accuracy. Although there is some previous research on the verification of angle measuring uncertainty for the rotary-laser system, there are still some limitations. High-precision reference angles are used in the study of the method, and an integrated verification platform is set up to evaluate the performance of the system. This paper also probes the error that has biggest influence on the verification system. Some errors of the verification system are avoided via the experimental method, and some are compensated through the computational formula and curve fitting. Experimental results show that the angle measurement performance meets the requirement for coordinate measurement. The verification platform can evaluate the uncertainty of angle measurement for the rotary-laser system efficiently. © The Authors. Published by SPIE under a Creative Commons Attribution 3.0 Unported License. Distribution or reproduction of this work in whole or in part requires full attribution of the original publication, including its DOI. [DOI: 10.1117/1.OE.57.4.044106]

Keywords: rotary-laser; large-scale measurement; angle measurement performance; error compensation; measurement uncertainty.

Paper 180277 received Feb. 21, 2018; accepted for publication Mar. 23, 2018; published online Apr. 26, 2018.

## 1 Introduction

The rotary-laser system is a large-scale distributed system based on the intersection of laser beams from multiple stations. The rotary-laser system<sup>1</sup> has been used accurately to measure large structures and has potential applications in robotics,<sup>2</sup> aircraft, shipbuilding, the assembly of large components,<sup>3</sup> and mobile platform calibrations.<sup>4</sup> The system combines the principle of the photoelectric scanning with the concept of large-scale volume measurement.<sup>5</sup> Coordinate calculation is conducted by the signal processor and terminal computer to obtain high-precision computation. The distributed measurement network allows multiple receivers to work simultaneously. The measurement range can be expanded by increasing the number of transmitters, and the expanded range can ensure that the uncertainty of local measurement meets that of the overall measurement at the same time. Accurate measurements could subsequently be used to automatically correct the processes and compensate for manufacturing errors.<sup>6</sup>

The rotary-laser system uses the principle of intersection to set up a plurality of plane equations through the angle acquired by the receiver. It is then possible for three-dimensional (3-D) coordinates to be calculated according to the space plane intersection constraint.<sup>5,7</sup> In the absence of an accurate goniometric auxiliary device, angle measurement performance is difficult to assess.

There has been a large body of literature studying commercial rotary-laser systems, which include the indoor Global Positioning System (iGPS) of Nikon and the workshop Measurement Positioning System (wMPS) of Tianjin University. Studies have verified the performance of iGPS through comparison with points calibrated using a network of laser trackers<sup>8,9</sup> and obtained coordinate measurement

accuracy through the principle of isolating subsystems. Since there is reference significance for angle measurement performance of the rotary-laser system, there is an urgent need to establish a standard for the angle verification. Hirt et al.<sup>10</sup> did some research on the accuracy of tilt measurements on a hexapod-based Digital Zenith Camera System (DZCS) and reached the conclusion that DZCS may be a suitable system for accurate tilt measurement. However, DZCS is unsuitable for the verification of the rotary-laser system. To analyze the angular uncertainties of rotary-laser automatic theodolite, the fundamental physics of the rotating head device may be used to propagate uncertainties using Monte Carlo simulation, and Muelaner et al.<sup>11</sup> found that the uncertainty in azimuth is considerably higher than the uncertainty in elevation. Muelaner et al. carried out experiments to determine the actual uncertainty in the azimuth angle using the reference cylinder and dial gauge, but the dial gauge method is so complicated that the operator has to adjust the cylinder again and again when the dial gauge is moved to different positions. Furthermore, the verification accuracy can be influenced by a mechanical error of the cylinder. Geng et al.<sup>12</sup> investigated the relationship among uncertainties of azimuth and the elevation angle and internal parameters of wMPS; the study provides a basis for the theoretical analysis of the angle verification. Chao et al.<sup>13</sup> and Zhi et al.<sup>14</sup> designed methods to verify the wMPS using the polyhedral prism and electronic auto-collimator. The adjustment device added to the rotating head is so heavy that it may negatively influence the shafting, and the process is too complex to do in a single day to verify a transmitter. However, this previous research has been essential for informing this study.

The key to verifying the angle measurement performance is ensuring that the virtual axis of rotation of the rotor system is highly coaxial with the rotation axis of the angle standard device. Unfortunately, the work published<sup>11,13,14</sup> for the

\*Address all correspondence to: Yongjie Ren, E-mail: [yongjieren@tju.edu.cn](mailto:yongjieren@tju.edu.cn)

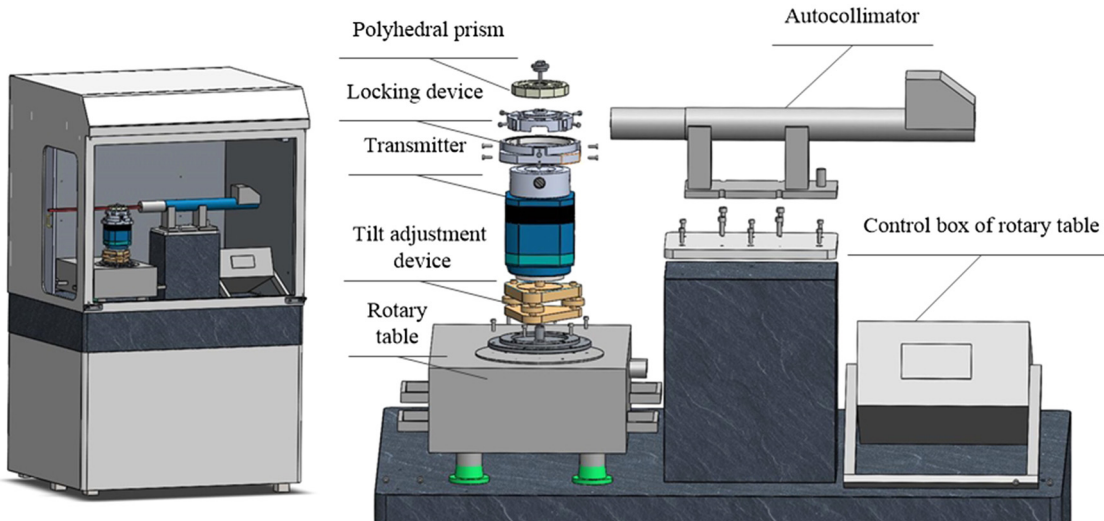


**Fig. 1** Design of azimuth accuracy verification platform.

verification of the rotary-laser system is not perfect enough. The objective of this paper is to devise an optimized verification method for the performance of the rotary-laser system. Multiple devices are integrated on a platform, and a verification system is devised. Additionally, this paper does in-depth research on the adjustment errors and system errors, finding that eccentricity contributes the most to the system through simulation. The error is compensated through the computational formula and curve fitting.

## 2 Experimental Methods

This test was carried out on the platform for verification. An optimized method was used to reach the goal of the experiment.

The multooth indexing rotary table was used to provide the angular standard, and the polyhedral prism, electronic autocollimator,<sup>15</sup> and tilt-adjustment device were used for assistance. There was an even number of working faces on the polyhedral prism. The polyhedral prism was put on the transmitter carefully via a light-fixing device, and a locking device was used to make sure the rotating head of the transmitter did not rotate. The tilt-adjustment device had two rotational degrees of freedom. All the devices were integrated on a unit of measurement platform (see Fig. 1).

The uncertainty in azimuth was obtained by comparing the measured azimuth angles with the rotation angles of the rotary table, and the uncertainty in elevation was obtained through the relationship between the azimuth angle and

elevation angle. The maximum angle error of the rotary table was 0.5 arc sec, the manufacturing tolerance of the polyhedral prism was  $\pm 1$  arc sec, and the angle measurement accuracy of the electronic autocollimator (TRIOPTICS TriAngle) was 0.4 arc sec.

The first procedure conducted was presetting the measurement device for the view angle of the electronic autocollimator to be  $<10$  arc sec. The transmitter replica, which was the same height as the real transmitter, was placed onto the tilt-adjustment device. The pitch of the electronic autocollimator and the dip of the tilt-adjustment device were adjusted slightly so that the electronic autocollimator could get reflection images clearly at each working surface of the polyhedral prism.

The second procedure was to adjust the pitch of the autocollimator. The polyhedral prism was simply placed on the head of the transmitter via a connector. Since this may have caused the polyhedral prism and the rotating head of the transmitter not to be parallel to each other, the pitch angle was adjusted slightly until the horizontal-direction angle readings in the opposite working surfaces of the polyhedral prism were equal and the vertical-direction angle readings were opposite when the rotary table turned 180 deg (see Fig. 2) without changing the dip of the tilt-adjustment device. After rotating 90 deg and fine-tuning the pitch, the angle readings in each working surface of the polyhedral prism were in tolerance (shown in the tips in the end of this section). The vector of the electronic autocollimator

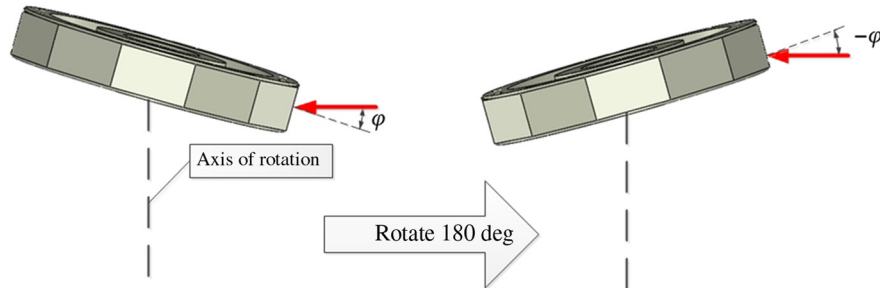


**Fig. 2** Diagram of exit rays of autocollimator.

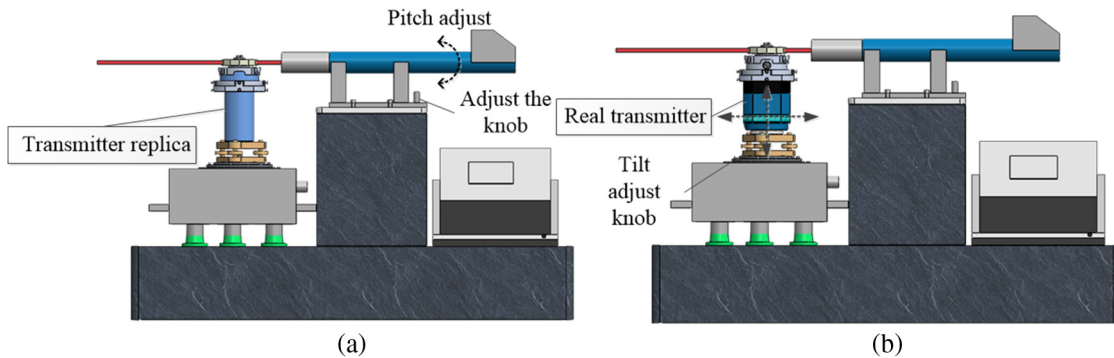


**Fig. 3** Schematic diagram of axis adjustment process: (a) procedure two: pitch adjust and (b) procedure three: tilt adjust.

projection and the axis of rotation of the rotary table were perpendicular to each other at the end of this procedure [see Fig. 3(a)].

The third procedure was replacing the transmitter replica with the real transmitter. The pitch of the electronic autocollimator was unchanged. The dip of the tilt-adjustment device was adjusted until the angle reading in the electronic autocollimator was the same as the second procedure. At this point, the axis of rotation of the rotary table and the axis of rotation of the transmitter are parallel to each other [see Fig. 3(b)].

The final procedure was placing the receiver about 10 m away from the transmitter and approximately in the  $x$ - $O$ - $y$  plane of the transmitter coordinate ( $z$ -value equals to zero). The data stream is provided by the processor.

Repeating the last two procedures was necessary only when another transmitter's accuracy needed to be verified.

This experimental process is shown in Fig. 4.

Tips: In the second and third procedures, when the horizontal-direction angle readings of the electronic autocollimator are  $<5$  arc sec in the opposite working surfaces of the polyhedral prism, regard them as “equal.” When the sums of the vertical-direction angle readings are between  $-10$  arc sec and  $10$  arc sec, regard them as “opposite.”

### 3 Error Analysis

In Sec. 2, we described the procedure for adjusting the axis of rotation of the transmitter. However, the prework may not be perfect and the axis of rotation of the transmitter was not

strictly parallel to the axis of the rotary table. Adjustment errors, such as axis tilt errors and eccentricity errors, may influence the final measurement uncertainty. When the verification experiment is carried out, the height of the receiver also influences the result.

#### 3.1 Axis Tilt Error

Axis tilt error represents the axis of rotation of the rotary table when it is not strictly parallel to the axis of rotation of the transmitter. The tilt angle of the transmitter rotation axis has an effect on the measurement azimuth angle. A base coordinate in the initial position of the rotary table is established as shown in Fig. 5, where  $\alpha_0$  and  $\beta_0$  represent the horizontal angle and vertical angle of the transmitter rotation axis, respectively. The rotation matrix between the base coordinate and the transmitter coordinate is calculated as

$$\begin{aligned} R_T &= \begin{bmatrix} Rx \\ Ry \\ Rz \end{bmatrix} = R_Y \cdot R_z \\ &= \begin{bmatrix} \cos(\frac{\pi}{2} - \beta_0) & 0 & \sin(\frac{\pi}{2} - \beta_0) \\ 0 & 1 & 0 \\ -\sin(\frac{\pi}{2} - \beta_0) & 0 & \cos(\frac{\pi}{2} - \beta_0) \end{bmatrix} \cdot \begin{bmatrix} \cos \alpha_0 & -\sin \alpha_0 & 0 \\ \sin \alpha_0 & \cos \alpha_0 & 0 \\ 0 & 0 & 1 \end{bmatrix} \\ &= \begin{bmatrix} \cos(\frac{\pi}{2} - \beta_0) \cdot \cos \alpha_0 & -\cos(\frac{\pi}{2} - \beta_0) \cdot \sin \alpha_0 & \sin(\frac{\pi}{2} - \beta_0) \\ \sin \alpha_0 & \cos \alpha_0 & 0 \\ -\sin(\frac{\pi}{2} - \beta_0) \cdot \cos \alpha_0 & \sin(\frac{\pi}{2} - \beta_0) \cdot \sin \alpha_0 & \cos(\frac{\pi}{2} - \beta_0) \end{bmatrix} \end{aligned} \quad (1)$$

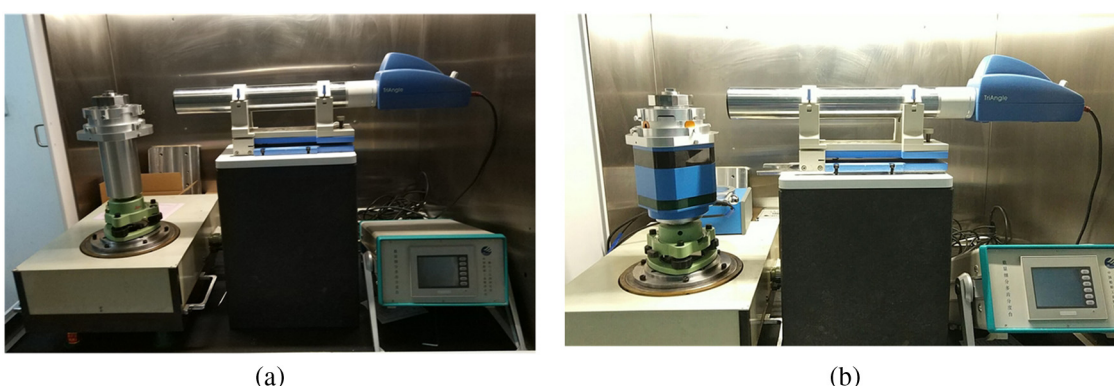


**Fig. 4** Image of experimental process: (a) electronic autocollimator pitch adjust and (b) transmitter tilt adjust.

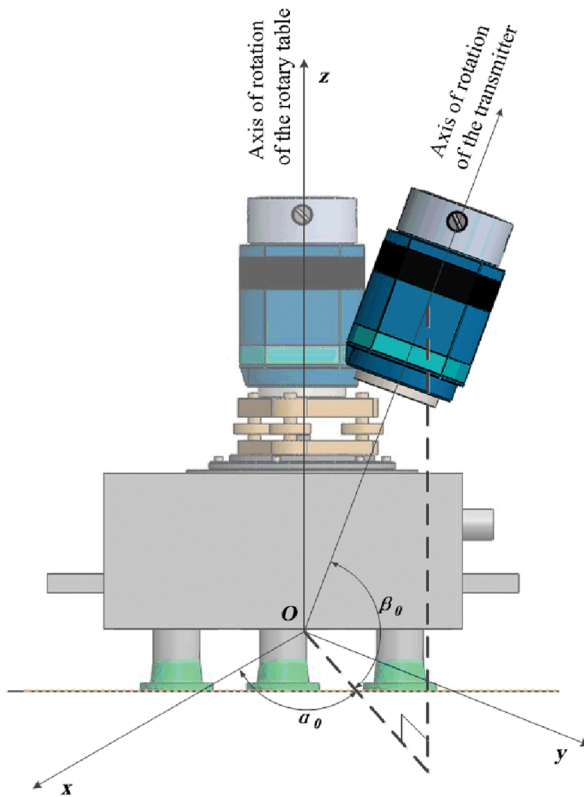


**Fig. 5** Schematic diagram of axis inclination of transmitter.

Assume that the receiver's position under the base coordinate is  $P = [X \ Y \ Z]^T$  and  $\alpha_0 = 0$ . The 3-D coordinates of the receiver in the transmitter coordinate are calculated as

$$P_0 = R_T \cdot P = \begin{bmatrix} \cos(\frac{\pi}{2} - \beta_0) & 0 & \sin(\frac{\pi}{2} - \beta_0) \\ 0 & 1 & 0 \\ -\sin(\frac{\pi}{2} - \beta_0) & 0 & \cos(\frac{\pi}{2} - \beta_0) \end{bmatrix} \cdot \begin{bmatrix} X \\ Y \\ Z \end{bmatrix}. \quad (2)$$

If the rotary table rotates at an angle  $\theta$ , the transmitter coordinate also rotates at an angle  $\theta$  around the  $z$ -axis of the base coordinate. The 3-D coordinates of the receiver under the transmitter coordinate are calculated as

$$P_1 = R_T \cdot \begin{bmatrix} \cos \theta & -\sin \theta & 0 \\ \sin \theta & \cos \theta & 0 \\ 0 & 0 & 1 \end{bmatrix} \cdot P = \begin{bmatrix} X_1 \\ Y_1 \\ Z_1 \end{bmatrix}. \quad (3)$$

The measured azimuth angle of the transmitter can be calculated easily by geometric projection and is calculated as

$$\alpha = \arctan\left(\frac{Y_1}{X_1}\right). \quad (4)$$

Assuming that the receiver is in the  $x$ - $O$ - $y$  plane and 10 m away from the transmitter, the angle error can be calculated when the tilt angle is given. As shown in Fig. 6, when the tilt angle of the transmitter rotation axis is 30 arc sec, the

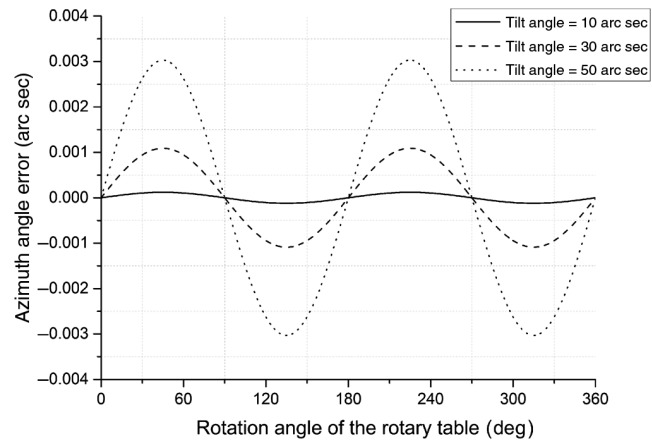


**Fig. 6** Effects of the tilt angle.

peak-to-valley error caused by the tilt is  $<0.003$  arc sec. When the angle is reduced to 10 arc sec, the error becomes 0.0003 arc sec.

As a result, if the tilt angle is small enough, the azimuth angle error can be ignored. It is acceptable to adjust the tilt angle of the transmitter rotation axis to a level  $<10$  arc sec.

### 3.2 Eccentricity Error

The eccentricity error is caused by the axis of rotation of the transmitter, and the axis of rotation of the rotary table is not adjusted to a coaxial position.

This error is shown in Fig. 7(a). Eccentricity error may be compensated for when the mathematical model of the error is given according to the geometric relationship [see Fig. 7(b)].

Assuming that the receiver is  $R$  meters away from the axis of rotation of the rotary table, the eccentricity between the axis of rotation of the rotary table and the axis of rotation of transmitter is  $d$ . The rotary table has rotated to an angle  $\theta$  relative to its initial setting.

The vector from the center of the rotary table to the receiver is given by

$$\overline{O_1 P} = [R \cos \theta \ R \sin \theta]. \quad (5)$$

The vector from the center of the transmitter to the receiver is given by

$$\overline{O_2 P} = [R \cos \theta - d \ R \sin \theta]. \quad (6)$$

It is straightforward to calculate the azimuth angle error caused by eccentricity; the error  $|\Delta\theta|$  (see Fig. 8) is calculated as

$$\begin{aligned} |\Delta\theta| &= \arccos\left(\frac{\overline{O_1 P} \Delta \overline{O_2 P}}{|\overline{O_1 P}| |\overline{O_2 P}|}\right) \\ &= \arccos\left(\frac{R - d \cos \theta}{\sqrt{R^2 - 2Rd \cos \theta + d^2}}\right). \end{aligned} \quad (7)$$

As shown in Fig. 7, when the eccentricity  $d$  is 0.1 mm, the maximum azimuth angle error caused by eccentricity is up to 2.06 arc sec. This is too large, and it must be compensated for.

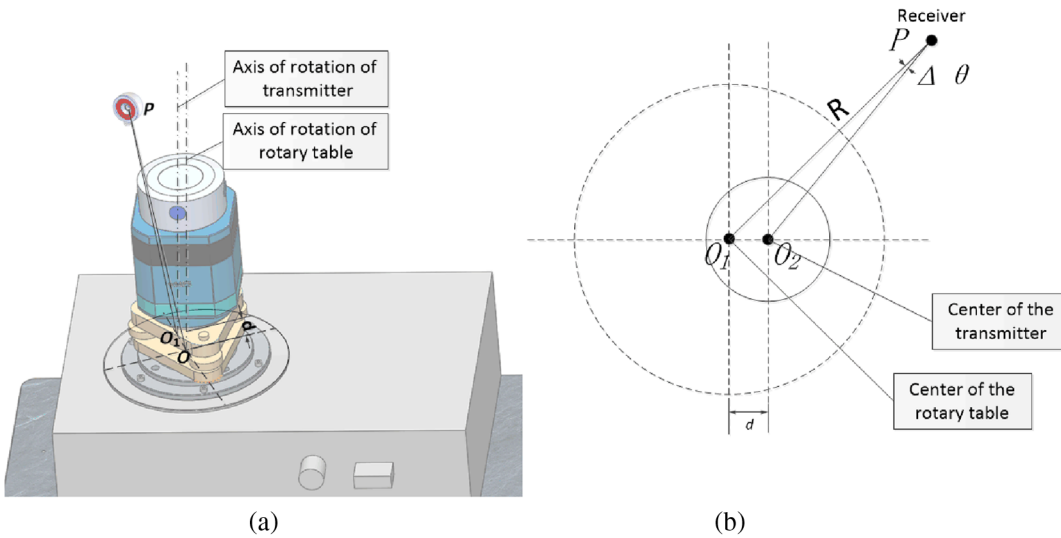


**Fig. 7** Effect of the eccentricity error: (a) stereo model of axis eccentricity and (b) schematic diagram of axis eccentricity.

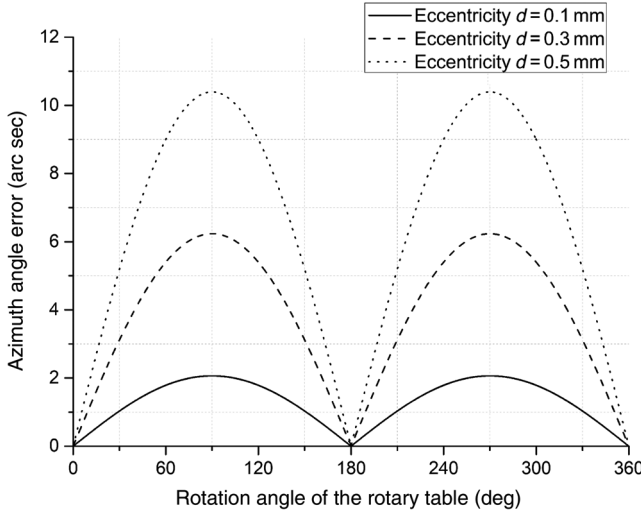


**Fig. 8** Change regulation caused by the eccentricity error.

### 3.3 Error Caused by the Height of the Receiver

The error caused by the height of the receiver ( $z$ -value) does not influence the result independently. In other words, when the receiver is not in the  $x$ - $O$ - $y$  plane and the axis tilt angle and eccentricity are zero, the result is not influenced. However, when the  $z$ -value becomes larger, the error analyzed in Secs. 3.1 and 3.2 increases. This error is related to the other two errors.

#### 3.3.1 Influence on the axis tilt error

The error level analyzed in Sec. 3.1 is premised on the receiver being in the  $x$ - $O$ - $y$  plane and the  $z$ -value being zero. However, the larger the height is, the larger the azimuth angle error is in the same rotation angle of the rotary table. In this test, a simulation was carried out regarding this problem.

If the tilt angle of the axis of rotation of the transmitter is 10 arc sec and the height of the receiver changes from 20 to 520 mm, the result is as shown in Fig. 9. When the height of

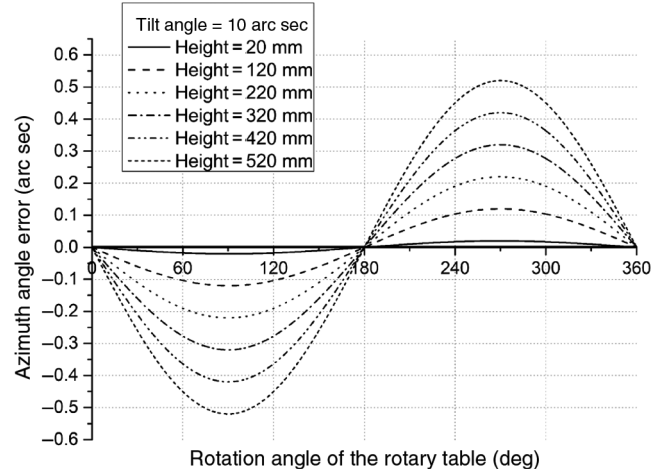


**Fig. 9** Influence on the axis tilt error of height of the receiver.

the receiver is  $<20$  mm, the maximum angle error caused by axis tilt error and the height of the receiver is  $<0.02$  arc sec. It is better to place the receiver near the  $x$ - $O$ - $y$  plane within 20 mm.

#### 3.3.2 Influence on the eccentricity error

The error analyzed in Sec. 3.2 is also calculated when the  $z$ -value equals zero. When the  $z$ -value increases, the error model caused by the height of the receiver is as shown in Fig. 10.

Point  $P_1$  is in the  $x$ - $O$ - $y$  plane and point  $P_2$  is  $h = 20$  mm higher than the  $x$ - $O$ - $y$  plane.

Assuming that the eccentricity  $d = 0.1$  mm and  $R = 10$  m, the maximum eccentricity error is  $\Delta\theta_1 = 2.0626$  arc sec when the receiver is placed in point  $P_1$ . When the receiver is placed in point  $P_2$ , the eccentricity error is  $\Delta\theta_1 = 2.0622$  arc sec, according to geometrical relations.

As a result, when the height of the receiver is  $<20$  mm, the error is small enough to be ignored.

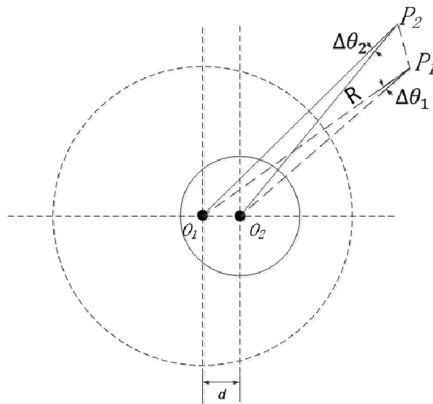


**Fig. 10** Influence on the eccentricity error of the height of the receiver.

### 3.4 Machining Error

Machining error is caused by the axis of rotation of the transmitter and does not strictly coincide with the axis of the rotating head of the transmitter. In the process of this experiment, the rotating head of the transmitter was locked onto the stationary body. The axis of rotation of the transmitter was used as the target of the experimental adjusting axis, which introduces machining error, because the transmitter is symmetrical. In fact, the axis of the rotating head should be adjusted, but it is more complicated to make the axis of the rotating head rotate the same angle as that of the rotary table. However, the transmitter was assembled with high precision, and the deviation of the axis of the rotation of the transmitter is small. Furthermore, the machining error analyzed in this section conforms to the axis tilt error model and the eccentricity error model supported by the theoretical analysis in Secs. 3.1 and 3.2. This error can be compensated along with the eccentricity error.

## 4 Results

### 4.1 Data Processing

The data stream includes  $t_1$ ,  $t_2$ , and  $T$ , where  $t_1$  and  $t_2$  represent the moment that the two scanning fans reach the receiver and  $T$  represents the transmitter's rotation period.

The measurement data were obtained from rotating the rotary table 10 deg counterclockwise each time and 540 deg in total. In the test, there were 54 packages of measurement data and 1530 measurement instances in each package. The average of each package was used to find the angle in each position.

The angle calculation formula is calculated as

$$\begin{cases} \Delta\varphi_{1(i)} = \theta_{1(i+1)} - \theta_{1(i)} = (t_{1(i+1)} - t_{1(i)}) * 2 \pi \\ \Delta\varphi_{2(i)} = \theta_{2(i+1)} - \theta_{2(i)} = (t_{2(i+1)} - t_{2(i)}) * 2 \pi \end{cases} \quad (8)$$

where  $i = 1, 2, \dots, 53$  and  $t_{1(i)}$  and  $t_{2(i)}$  represent the moment that two scanning fans reached the receiver at the angle  $10 \cdot (i-1)$  deg.  $\Delta\varphi_{1(i)}$  and  $\Delta\varphi_{2(i)}$  represent the difference between the two measured rotation angles at  $10 \cdot (i-1)$  deg and  $10 \cdot i$  deg, which were obtained by the two fans, respectively.

The receiver is placed approximately in the horizontal plane of the transmitter coordinate  $x$ - $O$ - $y$ ; the  $z$ -value (the elevation angle) may not be equal to zero. Though the measured rotation angle is not strictly equal to the azimuth angle, the change in the angle is the same. Finally, the azimuth angle error is obtained by the subtraction of the measured rotation angle.

The following discussion is based on the data regarding the first fan of the transmitter  $\Delta\varphi_{1(i)}$ .

It is clear that the data (see in Fig. 11) comply with the obvious law of sinusoidal variation and the law of the eccentricity error model discussed in Sec. 3 in this paper.

The sinusoidal equation can be determined according to the curve fitting method when processing the data. The fitting equation is given by

$$f(x) = a_1 \sin(b_1 x + c_1) + a_2 \sin(b_2 x + c_2). \quad (9)$$

The result of this fitting in MATLAB™ is calculated as Eq. (10). The RMSE is 0.82, and the red curve in Fig. 11 is the residual, which is the difference between the raw data and the fitted data. The model's results were in good agreement with the experimental data.

$$\begin{aligned} f(x) = & 4.515 * \sin(0.1926 * x + 0.1506) + 37.46 \\ & * \sin(0.172 * x + 0.9758). \end{aligned} \quad (10)$$

### 4.2 Error Compensation

In the test, the distance  $R$  from the receiver to the axis of rotation of the rotary table was 9.9222 m. The maximum azimuth angle error can be calculated using the fitting curve and  $|\Delta\varphi_{i\text{MAX}}| = 41.75$  arc sec. According to Eq. (7), the eccentricity is  $d = 2.0085$  mm, and the eccentricity error needs to be compensated for.

The raw data curve is moved horizontally so that the zero of the raw data and the zero in Eq. (7) coincide. The adjusted azimuth angle error is calculated by subtracting the raw data from the calculated system error in Eq. (7). The result is shown in Fig. 12.

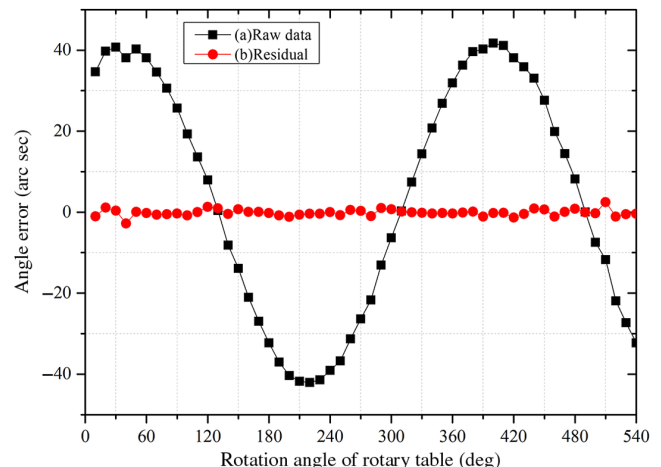


**Fig.11** Raw data curve and residual curve.

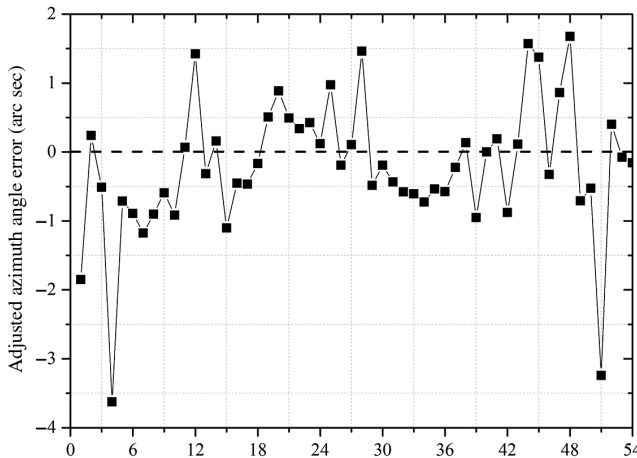


**Fig.12** Measurement uncertainty of the azimuth angle.

## 5 Discussions

### 5.1 Uncertainty in Azimuth

The factors that contribute to the uncertainty are as follows: (a) the uncertainty of curve fitting when compensating the eccentricity error, (b) the uncertainty caused by adjustment error, which means the axis tilt error, and (c) the measurement uncertainties of the instruments caused by the rotary table, the polyhedral prism, and the autocollimator.

In all tests, it was found that the  $z$ -value of the receiver was  $<20$  mm and the axis tilt error was adjusted to  $<10$  arc sec. The maximum azimuth angle error is 0.04 arc sec, and, therefore, the uncertainty caused by the axis tilt error is  $u_1 = 0.04$  arc sec.

The system errors were ignored after compensation, but the uncertainty of curve fitting was introduced. According to the curve fitting evaluation, the RMSE is 0.82. RMSE represents the level of the deviation between the measurement value and the true value. In other words, it also represents the level of azimuth angle error. The level of RMSE (0.82) is conformable to reality in engineering applications of the rotary-laser systems. As a result, the uncertainty of the curve fitting can be ignored.

The uncertainties of the polyhedral prism and electronic autocollimator have little influence on the adjustment error and may be  $<0.01$  arc sec. This error can be ignored. The uncertainty of the rotary table should use the assessment

method of the type B uncertainty component. The maximum angle error of the rotary table is 0.5 arc sec. As a result, the uncertainty caused by the instruments is  $u_2 = 0.5$  arc sec /  $\sqrt{3} = 0.35$  arc sec, assuming that the error obeys uniform distribution

$$\begin{aligned} S &= \sqrt{\frac{\sum_{i=1}^n (x_i - \bar{x})^2}{n-1}} \\ &= \sqrt{\frac{(x_1 - \bar{x})^2 + (x_2 - \bar{x})^2 + \dots + (x_n - \bar{x})^2}{n-1}}. \end{aligned} \quad (11)$$

According to the Bessel formula [see Eq. (11)], the standard deviation of the adjusted azimuth angle error is 0.98 arc sec, and the standard uncertainty of the adjusted azimuth angle error is  $u_\varphi = S = 0.98$  arc sec. The relationship between the adjusted azimuth angle error and the measured angle is calculated as Eq. (8). According to the guide to the expression of uncertainty in measurement,<sup>16</sup> the relationship of uncertainty between them is given by

$$u_\varphi^2 = u_{\theta_{1(i+1)}}^2 + u_{\theta_{1(i)}}^2. \quad (12)$$

Combined with  $u_{\theta_{1(i+1)}} = u_{\theta_{1i}}$ , the standard uncertainty in azimuth may be arranged as

$$u_3 = u_\varphi / \sqrt{2} = 0.69 \text{ arc sec}. \quad (13)$$

The combined uncertainty of the azimuth angle is calculated as

$$u_{c1} = \sqrt{u_1^2 + u_2^2 + u_3^2} = 0.77 \text{ arc sec}. \quad (14)$$

### 5.2 Uncertainty in Elevation

The uncertainty of the elevation angle is obtained through the relationship between the azimuth angle and elevation angle and shows that relationship between uncertainties of the two angles can be calculated.<sup>17-19</sup> The elevation angle is calculated as

$$\beta = \arctan \left[ \frac{\sin(\theta_1 - \alpha)}{\tan \varphi_1} \right]. \quad (15)$$

A differential operation is applied to Eq. (15) and calculated as

$$d\beta = \frac{\cos(\theta_1 - \alpha) \tan \varphi_1 d\theta_1 - \cos(\theta_1 - \alpha) \tan \varphi_1 d\alpha - \sin(\theta_1 - \alpha) \sec \varphi_1^2 d\varphi_1}{\tan \varphi_1^2 + \sin(\theta_1 - \alpha)^2}. \quad (16)$$

The internal parameter  $\varphi_1$  remained unchanged when the verification method was carried out, and the covariance of  $\beta$  is calculated as

$$\sigma_\beta = \frac{-\cos(\theta_1 - \alpha) \tan \varphi_1 \sigma_\alpha}{\tan \varphi_1^2 + \sin(\theta_1 - \alpha)^2}. \quad (17)$$

The rotation angle  $\theta_1$  approximately equals the azimuth angle  $\alpha$  for the receiver and is placed near the  $x$ - $O$ - $y$

plane, meaning that  $\cos(\theta_1 - \alpha) \approx 1$  and  $\sin(\theta_1 - \alpha) \approx 0$ . Combined with  $\varphi_1 = 0.8319$ , the covariance of the elevation angle is  $\sigma_\beta = 0.55$  arc sec. The uncertainty in elevation is  $u_{c2} = \sigma_\beta = 0.70$  arc sec.

As a fact,  $\cos(\theta_1 - \alpha) < 1$  and  $\sin(\theta_1 - \alpha) \neq 0$ ; uncertainty of the elevation angle is  $<0.55$  arc sec.

As a result, the expanded uncertainty of the azimuth angle is 1.5 arc sec and the elevation angle is  $<1.4$  arc sec. This is calculated using a coverage factor of 2 (which is related to a level of confidence of  $\sim 95.45\%$ ).

## 6 Conclusions

In this paper, a unit of verification platform was designed to verify the angle performance of the rotary-laser system. This platform can be easily used for the verification of the next transmitter without rebuilding the experimental environment. The adjustment error and system error models were analyzed in detail. The axis tilt error and the error caused by the height of the receiver have little influence on the results when the receiver is placed in the proper position. The concentric adjustment, which introduces system errors, was omitted through compensation and the result was as expected. The experiments indicate that the level of uncertainty of the azimuth angle was  $\sim 1.5$  arc sec and the uncertainty of the elevation angle was  $<1.4$  arc sec at a 95.45% level of confidence. The results indicate that the transmitters meet the measurement requirements. This verification unit may gradually form a standard to verify the performance of the angle measurement of rotary-laser systems.

Future research will focus on adjusting the axis of the rotating head of the transmitter coaxial with the axis of rotation of the rotary table to verify the performance of the rotary-laser system more precisely. A study to verify the angle performance of the rotary-laser system will be carried on and the measurement accuracy of the rotary-laser system will be improved in the future.

## Acknowledgments

This work was supported by the National Natural Science Foundation of China (Grant Nos. 51475329 and 51775380), the National Key Research and Development Project of China (Grant No. 2017YFF0204802), the Foundation for Innovative Research Groups of the National Natural Science Foundation of China (Grant No. 51721003), and the Young Elite Scientists Sponsorship Program by China Association for Science and Technology (Grant No. 2016QNRC001).

## References

- C. Depenthal and J. Schwendemann, "iGPS—a new system for static and kinematic measurements," *Opt. 3-D Meas. Tech. IX* **1**(1–3), 131–140 (2009).
- R. Schmitt et al., "Performance evaluation of iGPS for industrial applications," in *Int. Conf. on Indoor Positioning and Indoor Navigation (IPIN)* (2010).
- R. Schmitt et al., "Investigation of the applicability of an iGPS metrology system to automate the assembly in motion of a truck cabin," *Appl. Mech. Mater.* **840**, 58–65 (2016).
- S. Kang and D. Tesar, "Indoor GPS metrology system with 3D probe for precision applications," in *Proc. of ASME Int. Mechanical Engineering Congress*, pp. 1–4 (2004).
- Z. Zhao et al., "Transmitter parameter calibration of the workspace measurement and positioning system by using precise three-dimensional coordinate control network," *Opt. Eng.* **53**(8), 084108 (2014).
- J. E. Muelaner et al., "Verification of the indoor GPS system by comparison with points calibrated using a network of laser tracker measurements," in *Proc. of 6th CIRP Sponsored Int. Conf. on Digital Enterprise Technology*, Vol. **66**, pp. 607–619 (2010).
- J. E. Muelaner et al., "Estimation of uncertainty in three-dimensional coordinate measurement by comparison with calibrated points," *Meas. Sci. Technol.* **21**(2), 025106 (2010).
- Y. Chen et al., "A structured light sensor measuring method based on wMPS global controlling," *Proc. SPIE* **9671**, 967105 (2015).
- D. Djurdjanovic and J. Ni, "Online stochastic control of dimensional quality in multistation manufacturing systems," *Proc. Inst. Mech. Eng. Part B J. Eng. Manuf.* **221**(5), 865–880 (2007).
- C. Hirt et al., "Expected accuracy of tilt measurements on a novel hexapod-based digital zenith camera system: a Monte-Carlo simulation study," *Meas. Sci. Technol.* **25**(8), 1408–1424 (2015).
- J. E. Muelaner et al., "Study of the uncertainty of angle measurement for a rotary-laser automatic theodolite (R-LAT)," *Proc. Inst. Mech. Eng. Part B J. Eng. Manuf.* **223**(3), 217–229 (2009).
- L. Geng et al., "Analysis of angle measurement uncertainty for wMPS," *Proc. SPIE* **7544**, 754403 (2010).
- D. Chao et al., "Evaluation method of angle measurement accuracy for wMPS" *Nano. Precis. Eng.* **15**(6), 466–472 (2018) (in Chinese).
- X. Zhi et al., "Verification of angle measuring uncertainty for workspace measuring and positioning system," *Chin. J. Sens. Actuators* **25**(2), 229–235 (2012) (in Chinese).
- J. Yuan and X. Long, "CCD-area-based autocollimator for precision small-angle measurement," *Rev. Sci. Instrum.* **74**(3), 1362–1365 (2003).
- IO Standardization, "Guide to the expression of uncertainty in measurement (GUM) general metrology, PD 6461–3 (1995).
- Z. Liu et al., "A single-station multi-tasking 3D coordinate measurement method for large-scale metrology based on rotary-laser scanning," *Meas. Sci. Technol.* **24**(10), 105004 (2013).
- Y. Xie et al., "A new single-station wMPS measurement method with distance measurement," *Proc. SPIE* **9677**, 96771Z (2015).
- N. Zhou et al., "iGPS measurement network multi-station arrangement design," *Appl. Mech. Mater.* **443**, 223–227 (2013).

**Jin Zhao** is a student at Tianjin University. He received his BS degree in measurement and control technology and instruments from Tianjin University in 2016, and he will receive his MS degree from Tianjin University in 2019. His current research interests include large-scale measurement and precision vision measurement.

**Yongjie Ren** received his PhD from Tianjin University in 2007. Currently, he is an associate professor at the State Key Laboratory of Precision Measurement Technology and Instruments, Tianjin University. His research interests are focused on industrial robot as well as vision measurement and photoelectric measuring technology.

**Jiarui Lin** received his PhD from Tianjin University in 2012. Currently, he is an associate professor at the State Key Laboratory of Precision Measurement Technology and Instruments, Tianjin University. His research interests include vision measurement and photoelectric measuring technology.

**Shibin Yin** received his PhD from Tianjin University in 2015. Currently, he is a lecturer at the State Key Laboratory of Precision Measurement Technology and Instruments, Tianjin University. His research interests include vision measurement and photoelectric measuring technology.

**Jigui Zhu** received his BS and MS degrees from the National University of Defense Science and Technology of China in 1991 and 1994, respectively, and his PhD from Tianjin University, China, in 1997. Currently, he is a professor at the State Key Laboratory of Precision Measurement Technology and Instruments, Tianjin University. His research interests include laser and photoelectric measuring technology, such as industrial online measurement and large-scale precision metrology.